



## Thermolysis of $\text{Fe}_3(\text{CO})_9(\mu_3\text{-Se})(\mu_3\text{-E})$ ( $\text{E} = \text{S}, \text{Te}$ ) with $\text{Cp}_2\text{Mo}_2(\text{CO})_6$ and formation of new mixed-chalcogenide, mixed Fe–Mo carbonyl clusters.

Crystal structures of  $\text{Cp}_2\text{Mo}_2\text{Fe}_2(\text{CO})_6(\mu_3\text{-Se})_2(\mu_4\text{-Te})$ ,  $\text{Cp}_2\text{Mo}_2\text{Fe}_2(\text{CO})_7(\mu_3\text{-Se})(\mu_3\text{-Te})$  and  $\text{Cp}_2\text{Mo}_2\text{Fe}_2(\text{CO})_6(\mu_3\text{-S})(\mu_3\text{-Se})(\mu_4\text{-Se})$

Pradeep Mathur <sup>a,\*</sup>, Sanjukta Ghose <sup>a</sup>, Md. Munkir Hossain <sup>a</sup>, C.V.V. Satyanarayana <sup>b</sup>,  
Mary F. Mahon <sup>c</sup>

<sup>a</sup> Chemistry Department, Indian Institute of Technology, Bombay 400 076, India

<sup>b</sup> Regional Sophisticated Instrumentation Centre, Indian Institute of Technology, Bombay 400 076, India

<sup>c</sup> School of Chemistry, University of Bath, Claverton Down, Bath BA2 7AY, UK

Received 28 January 1997

### Abstract

The thermolytic reaction of  $\text{Fe}_3(\text{CO})_9(\mu_3\text{-Se})(\mu_3\text{-Te})$  with  $\text{Cp}_2\text{Mo}_2(\text{CO})_6$  in benzene yielded the new mixed-metal, mixed trichalcogenide clusters  $\text{Cp}_2\text{Mo}_2\text{Fe}_2(\text{CO})_6(\mu_3\text{-Se})(\mu_3\text{-Te})(\mu_4\text{-Te})$  (**2a**),  $\text{Cp}_2\text{Mo}_2\text{Fe}_2(\text{CO})_6(\mu_3\text{-Te})_2(\mu_4\text{-Se})$  (**2b**) and  $\text{Cp}_2\text{Mo}_2\text{Fe}_2(\text{CO})_6(\mu_3\text{-Se})_2(\mu_4\text{-Te})$  (**3a**),  $\text{Cp}_2\text{Mo}_2\text{Fe}_2(\text{CO})_6(\mu_3\text{-Se})(\mu_3\text{-Te})(\mu_4\text{-Se})$  (**3b**) as well as the dichalcogenide cluster  $\text{Cp}_2\text{Mo}_2\text{Fe}_2(\text{CO})_7(\mu_3\text{-Se})(\mu_3\text{-Te})$  (**8**). Similarly, the thermolysis of  $\text{Fe}_3(\text{CO})_9(\mu_3\text{-S})(\mu_3\text{-Se})$  with  $\text{Cp}_2\text{Mo}_2(\text{CO})_6$  in benzene afforded the new mixed-metal, mixed trichalcogenide clusters  $\text{Cp}_2\text{Mo}_2\text{Fe}_2(\text{CO})_6(\mu_3\text{-S})_2(\mu_4\text{-Se})$  (**10**),  $\text{Cp}_2\text{Mo}_2\text{Fe}_2(\text{CO})_6(\mu_3\text{-S})(\mu_3\text{-Se})(\mu_4\text{-Se})$  (**11**) and the dichalcogenide cluster  $\text{Cp}_2\text{Mo}_2\text{Fe}_2(\text{CO})_6(\mu_3\text{-S})(\mu_3\text{-Se})$  (**13**). In the case of **10** and **11**, formation of isomers containing the sulphido in the  $\mu_4$ -site was not observed. Compounds **2a** and **2b** could also be obtained when  $\text{Cp}_2\text{Mo}_2\text{Fe}_2(\text{CO})_6(\mu_3\text{-Te})_2$  was refluxed with selenium powder in benzene. Similarly, refluxing of benzene solutions containing selenium powder and  $\text{Cp}_2\text{Mo}_2\text{Fe}_2(\text{CO})_6(\mu_3\text{-Se})(\mu_3\text{-Te})$  formed **3a** and **3b**, and sulphur powder with  $\text{Cp}_2\text{Mo}_2\text{Fe}_2(\text{CO})_6(\mu_3\text{-S})(\mu_3\text{-Se})$  or  $\text{Cp}_2\text{Mo}_2\text{Fe}_2(\text{CO})_6(\mu_3\text{-Se})_2$  yielded the compounds **10** and **11** respectively. The new clusters have been characterised by IR and by  $^1\text{H}$ ,  $^{13}\text{C}$ ,  $^{77}\text{Se}$  and  $^{125}\text{Te}$  NMR spectroscopy. Clusters **3a**, **8** and **11** have also been structurally characterised by single-crystal X-ray diffraction methods. © 1997 Elsevier Science S.A.

**Keywords:** Clusters; Iron; Molybdenum; Sulphur; Selenium; Tellurium

### 1. Introduction

The synthesis of high nuclearity transition metal carbonyl cluster compounds, by incorporating single atom ligands derived from certain main group elements of the Periodic Table, continues to be of considerable interest [1]. The importance of such compounds stems from the potential usefulness of the main group elements as bridges between the different early and late transition metal atoms in the clusters and as stabilising

ligands to prevent degradative fragmentation [2], to which such clusters are often susceptible, when subjected to rigorous conditions used during catalytic processes. The use of chalcogen atoms as bridging and stabilising ligands is now well established [3].

We have been interested in developing facile synthetic methods for preparation of heterochalcogen atom stabilised mixed-metal cluster compounds as they provide a unique opportunity to study the influence of the different chalcogen atoms on the structure, reactivity and bonding pattern of these complexes. The  $\text{Fe}_3(\text{CO})_9(\mu_3\text{-E})_2$  compounds, (where, E = S, Se or Te) have been used as convenient starting materials for this

\* Corresponding author.

Table 1  
Crystal data and details of measurements for compounds **3a**, **8** and **11**

Compound	<b>3a</b>	<b>8</b>	<b>11</b>
Formula	$C_{16}H_{10}Fe_2Mo_2O_6Se_2Te$	$C_{17}H_{10}Fe_2Mo_2O_7SeTe$	$C_{16}H_{10}Fe_2Mo_2O_6SSe_2$
Formula weight	887.34	836.39	791.8
Temperature (K)	293(2)	293(2)	293(2)
Wavelength (Å)	0.70930	0.70930	0.70930
Crystal system	Monoclinic	Orthorhombic	Orthorhombic
P2 <sub>1</sub> /n	0.2 × 0.2 × 0.2	0.2 × 0.15 × 0.15	<i>Cmcm</i> (No. 63) 0.3 × 0.3 × 0.25
Space group			
Crystal dimensions (mm <sup>3</sup> )			
<i>a</i> (Å)	10.418(4)	12.097(2)	10.455(1)
<i>b</i> (Å)	35.661(9)	12.739(2)	12.774(1)
<i>c</i> (Å)	12.553(4)	13.490(2)	15.392(1)
$\beta$ (deg)	112.34(2)	—	—
<i>U</i> (Å <sup>3</sup> )	4313.6(24)	2111.5(6)	2055.6(3)
<i>Z</i>	8	4	4
<i>D</i> (calc) (g cm <sup>-3</sup> )	2.733	2.631	2.56
<i>F</i> (000)	3280	1560	1376
$\mu(MoK\alpha)$ (mm <sup>-1</sup> )	7.186	5.622	6.25
$\theta$ range for data collection (deg)	2.09 to 23.95	2.26 to 23.92	3.18 to 23.92
Index ranges	$h = -11$ to +11, $k = 0$ to 40, $l = 0$ to 14	$h = 0$ to 13, $k = 0$ to 14, $l = 0$ to 15	$h = 0$ to 11, $k = 0$ to 14, $l = 0$ to 17
No. of reflections observed	6628	1740	878
No. of independent reflections ( $R(\text{int}) = 0.0000$ )	6628	1740	878
Data/restraints/parameters	6611/0/580	1739/1/291	875/0/84
Goodness-of-fit on $F^2$	0.651	0.651	0.863
Final <i>R</i> indices ( $I > 2\sigma(I)$ )	$R_1 = 0.0415$ <i>wR</i> 2 = 0.0966	$R_1 = 0.0230$ <i>wR</i> 2 = 0.0594	$R_1 = 0.0302$ <i>wR</i> 2 = 0.0841
<i>R</i> indices (all data)	$R_1 = 0.0825$ <i>wR</i> 2 = 0.1166	$R_1 = 0.0284$ <i>wR</i> 2 = 0.0682	$R_1 = 0.0397$ <i>wR</i> 2 = 0.0966
Largest diffracting, peak and hole (e <sup>-</sup> Å <sup>-3</sup> )	1.025 and -0.726	0.596 and -0.886	0.816 and -0.568
Maximum, minimum transmission corrections	1.000, 0.508	1.000, 0.708	1.000, 0.330
Weighting scheme, $w_c$	$1/[\sigma^2(F_o^2) + (0.0549P)^2 + 27.1957P]$ where $P = (F_o^2 + 2F_c^2)/3$ 0.0003(2)	$1/[\sigma^2(F_o^2) + (0.0718P)^2 + 21.3886P]$ where $P = (F_o^2 + 2F_c^2)/3$ 0.0017(2)	$1/[\sigma^2(F_o^2) + (0.0846P)^2 + 13.7568P]$ where $P = (F_o^2 + 2F_c^2)/3$ 0.0000(4)
Extinction coefficient			

The refinement method used in the case of all the three compounds was full-matrix least squares on  $F^2$ .

**Table 2**  
Atomic coordinates ( $\times 10^4$ ) and equivalent isotropic displacement parameters ( $\text{\AA}^2 \times 10^3$ ) for **3a**

Atom	x	y	z	$U_{\text{eq}}$ <sup>a</sup>
Te(1)	8430(1)	368(1)	9213(1)	34(1)
Se(1)	7952(1)	1130(1)	6886(1)	36(1)
Se(2)	6016(1)	400(1)	5964(1)	33(1)
Te(2)	8400(1)	1880(1)	4788(1)	33(1)
Se(3)	5161(1)	2338(1)	2378(1)	31(1)
Se(4)	7068(1)	1827(1)	1448(1)	39(1)
Mo(1)	6495(1)	781(1)	7751(1)	29(1)
Mo(2)	8541(1)	447(1)	7189(1)	30(1)
Mo(3)	7754(1)	2314(1)	2989(1)	30(1)
Mo(4)	6193(1)	1692(1)	3003(1)	30(1)
Fe(1)	9314(2)	1052(1)	8851(1)	34(1)
Fe(2)	6429(2)	–22(1)	7501(1)	34(1)
Fe(3)	6119(2)	2311(1)	4424(1)	34(1)
Fe(4)	8941(2)	1579(1)	3011(1)	42(1)
O(1)	11918(11)	1198(3)	8581(10)	79(3)
O(2)	10905(10)	933(3)	11316(8)	71(3)
O(3)	8540(9)	1804(2)	9346(8)	57(2)
O(4)	3423(10)	–116(3)	6759(10)	81(3)
O(5)	6776(12)	–455(3)	9577(9)	83(3)
O(6)	7102(10)	–657(2)	6323(8)	62(2)
O(7)	6812(10)	3098(2)	5010(8)	60(2)
O(8)	3250(10)	2269(3)	4242(9)	83(3)
O(9)	6941(12)	2091(3)	6840(9)	79(3)
O(10)	11218(14)	1285(5)	5029(11)	132(6)
O(11)	8290(14)	827(3)	2009(13)	117(5)
O(12)	10898(10)	1845(3)	2031(10)	81(3)
C(1)	5745(26)	1243(8)	8695(35)	72(16)
C(2)	5359(33)	890(10)	9006(18)	56(11)
C(3)	4353(27)	728(5)	8004(37)	82(17)
C(4)	4117(32)	980(11)	7073(18)	82(18)
C(5)	4977(41)	1298(7)	7500(36)	62(12)
C(1A)	5638(28)	1073(11)	9021(14)	49(14)
C(2A)	4809(34)	754(7)	8531(34)	25(7)
C(3A)	4135(25)	816(8)	7328(31)	56(15)
C(4A)	4548(32)	1173(9)	7074(16)	53(13)
C(5A)	5477(29)	1332(5)	8120(32)	44(12)
C(6)	10008(17)	–49(4)	7173(16)	73(5)
C(7)	9116(13)	19(4)	6065(13)	60(4)
C(8)	9380(14)	368(4)	5738(12)	57(3)
C(9)	10449(14)	527(4)	6682(14)	60(4)
C(10)	10838(14)	266(5)	7582(13)	72(5)
C(11)	10891(14)	1143(4)	8686(12)	56(3)
C(12)	10252(13)	957(3)	10355(11)	48(3)
C(13)	8846(12)	1510(3)	9151(10)	42(3)
C(14)	4627(15)	–76(4)	7054(12)	56(3)
C(15)	6719(15)	–268(3)	8788(12)	59(4)
C(16)	6877(12)	–409(3)	6812(11)	46(3)
C(17)	9866(15)	2633(4)	3399(17)	79(5)
C(18)	9174(16)	2613(4)	2206(15)	65(4)
C(19)	7959(17)	2819(4)	1886(13)	63(4)
C(20)	7870(15)	2958(3)	2861(14)	58(4)
C(21)	9047(17)	2849(4)	3827(12)	65(4)
C(22)	4067(18)	1467(5)	2881(34)	34(10)
C(23)	5053(29)	1314(6)	3912(22)	25(7)
C(24)	5960(22)	1078(6)	3611(13)	36(9)
C(25)	5535(24)	1085(7)	2394(14)	50(11)
C(26)	4365(23)	1325(6)	1943(20)	41(10)
C(22A)	4439(43)	1420(8)	3469(33)	44(11)
C(23A)	5586(35)	1172(12)	3907(27)	105(27)
C(24A)	5851(37)	1025(6)	2958(58)	108(25)
C(25A)	4868(54)	1183(10)	1935(30)	69(17)

Table 2 (continued)

Atom	x	y	z	$U_{\text{eq}}$ <sup>a</sup>
C(26A)	3995(22)	1427(9)	2251(30)	45(10)
C(27)	6512(12)	2792(3)	4748(10)	44(3)
C(28)	4380(14)	2286(4)	4289(11)	54(3)
C(29)	6720(13)	2163(3)	5897(11)	46(3)
C(30)	10301(18)	1407(5)	4291(14)	79(5)
C(31)	8556(18)	1127(4)	2423(16)	79(5)
C(32)	10121(13)	1737(4)	2415(12)	56(3)

<sup>a</sup>  $U_{\text{eq}}$  is defined as one-third of the trace of the orthogonalized  $U_{ij}$  tensor.

purpose [4]. It has been reported by Lesch and Rauchfuss that there is a sharp contrast in reactivity between  $\text{Fe}_3(\text{CO})_9(\mu_3\text{-Te})_2$  and  $\text{Fe}_3(\text{CO})_9(\mu_3\text{-S})_2$  or  $\text{Fe}_3(\text{CO})_9(\mu_3\text{-Se})_2$  towards a variety of Lewis bases [5]. Although the compound  $\text{Fe}_3(\text{CO})_9(\mu_3\text{-Te})_2$  can form Lewis base adducts of the form  $\text{Fe}_2(\text{CO})_6(\mu_3\text{-Te})_2\text{Fe}(\text{CO})_3\text{L}$ , its S<sub>2</sub> and Se<sub>2</sub> analogues do not give the corresponding adducts. A similar reactivity difference is also observed for  $\text{Fe}_2(\text{CO})_6(\mu\text{-E}_2)$  for different E ligands (E = S, Se, Te). The reaction of  $\text{Fe}_2(\text{CO})_6(\mu\text{-S}_2)$  with  $\text{Cp}_2\text{Mo}_2(\text{CO})_4$  is reported to form the cis-'Braunstein' and trans-'Curtis' isomers of  $\text{Cp}_2\text{Mo}_2\text{Fe}_2\text{S}_2(\text{CO})_8$  [6]. On the other hand,  $\text{Fe}_2(\text{CO})_6(\mu\text{-Se}_2)$  reacts with  $\text{Cp}_2\text{Mo}_2(\text{CO})_4$  to form  $\text{Cp}_2\text{Mo}_2\text{Fe}_2(\text{CO})_6(\mu_4\text{-Se})(\mu_3\text{-Se})_2$  and  $\text{Cp}_2\text{Mo}_2\text{Fe}_2(\text{CO})_7(\mu_3\text{-Se})_2$  [7].

Previously we have reported on the preparations of the mixed-chalcogenide clusters  $\text{Cp}_2\text{Mo}_2\text{Fe}_2(\text{CO})_6(\mu_4\text{-Te})(\mu_3\text{-S})(\mu_3\text{-E})$  (E = S, Se, Te) and observed that in all such clusters the quadruply bridging site was occupied by the Te ligand [7,8]. We wished to extend this study to other chalcogen combinations, primarily to investigate whether the quadruply bridging site would always be occupied by Te preferentially over S and Se. Here, we report on the synthesis and characterisation of the mixed chalcogenide clusters  $\text{Cp}_2\text{Mo}_2\text{Fe}_2(\text{CO})_6(\mu_3\text{-Te})(\mu_3\text{-Se})(\mu_4\text{-Te})$ ,  $\text{Cp}_2\text{Mo}_2\text{Fe}_2(\text{CO})_6(\mu_3\text{-Te})_2(\mu_4\text{-Se})$ ,  $\text{Cp}_2\text{Mo}_2\text{Fe}_2(\text{CO})_6(\mu_3\text{-Se})_2(\mu_4\text{-Te})$ ,  $\text{Cp}_2\text{Mo}_2\text{Fe}_2(\text{CO})_6(\mu_3\text{-Se})(\mu_3\text{-Te})(\mu_4\text{-Se})$ ,  $\text{Cp}_2\text{Mo}_2\text{Fe}_2(\text{CO})_6(\mu_3\text{-S})_2(\mu\text{-Se})$ ,  $\text{Cp}_2\text{Mo}_2\text{Fe}_2(\text{CO})_6(\mu_3\text{-Se})(\mu_3\text{-S})(\mu_4\text{-Se})$ ,  $\text{Cp}_2\text{Mo}_2\text{Fe}_2(\text{CO})_7(\mu_3\text{-Se})(\mu_3\text{-Te})$  and  $\text{Cp}_2\text{Mo}_2\text{Fe}_2(\text{CO})_7(\mu_3\text{-S})(\mu_3\text{-Se})$ , and establish a general trend for the preference of different chalcogen ligands between the  $\mu_3$ - and  $\mu_4$ -sites.

## 2. Experimental section

### 2.1. General procedures

All reactions and other manipulations were carried out using standard Schlenk techniques under an inert atmosphere of argon. All solvents were deoxygenated immediately prior to use. IR spectra were recorded on a

Nicolet 5DXB or Impact 400 FTIR spectrophotometer, as hexane or dichloromethane solutions in 0.1 mm path-length NaCl cells. Elemental analyses were performed using a Carlo-Erba automatic analyser.  $^1\text{H}$ ,  $^{13}\text{C}$ ,  $^{77}\text{Se}$  and  $^{125}\text{Te}$  NMR spectra were recorded on a Varian VXR-300S spectrometer in  $\text{CDCl}_3$ . The operating frequency for  $^{77}\text{Se}$  NMR was 57.23 MHz with pulse width of 15  $\mu\text{s}$  and a delay of 1 s. The operating frequency for  $^{125}\text{Te}$  NMR was 94.705 MHz with pulse width of 9.5  $\mu\text{s}$  and a delay of 1 s.  $^{77}\text{Se}$  NMR spectra are referenced to  $\text{Me}_2\text{Se}$  ( $\delta = 0$ ) and  $^{125}\text{Te}$  NMR spectra are referenced to  $\text{Me}_2\text{Te}$  ( $\delta = 0$ ). The starting materials  $\text{Cp}_2\text{Mo}_2(\text{CO})_6$  [9],  $\text{Fe}_3(\text{CO})_9(\mu_3\text{-Se})(\mu_3\text{-Te})$  [10],  $\text{Fe}_3(\text{CO})_9(\mu_3\text{-Te})_2$  [11] and  $\text{Fe}_3(\text{CO})_9(\mu_3\text{-S})(\mu_3\text{-Se})$  [12] were prepared as reported in the literature.

## 2.2. Thermolytic reaction of $\text{Fe}_3(\text{CO})_9\text{SeTe}$ with $\text{Cp}_2\text{Mo}_2(\text{CO})_6$

A mixture of  $\text{Cp}_2\text{Mo}_2(\text{CO})_6$  (0.3 g, 0.61 mmol) and  $\text{Fe}_3(\text{CO})_9(\mu_3\text{-Se})(\mu_3\text{-Te})$  (0.55 g, 0.88 mmol) in 100 ml

Table 3  
Atomic coordinates ( $\times 10^4$ ) and equivalent isotropic displacement parameters ( $\text{\AA}^2 \times 10^3$ ) for 8

Atom	<i>x</i>	<i>y</i>	<i>z</i>	$U_{\text{eq}}^{\text{a}}$
Mo(1)	-631(1)	33(1)	-1177(1)	22(1)
Mo(2)	345(1)	-1399(1)	-2524(1)	25(1)
Se(1)	1293(8)	-819(7)	-863(8)	37(2)
Te(1')	1212(9)	-853(6)	-923(8)	25(2)
Te(1)	-1618(3)	-608(2)	-2796(3)	29(1)
Se(1')	-1684(10)	-565(10)	-2790(8)	51(4)
Fe(1)	1420(1)	508(1)	-2077(1)	31(1)
Fe(2)	-191(1)	634(1)	-3157(1)	31(1)
O(1)	1542(9)	2213(10)	-3522(9)	75(3)
O(2)	3481(8)	-69(10)	-3035(9)	78(3)
O(3)	2564(9)	2024(9)	-842(9)	72(3)
O(4)	230(10)	111(9)	-5236(6)	68(3)
O(5)	-1506(8)	2422(9)	-3718(6)	60(3)
O(6)	-222(7)	2370(6)	-1448(7)	44(2)
O(7)	-963(8)	-2815(7)	-1048(7)	53(2)
C(1)	1153(11)	1507(11)	-3120(10)	48(3)
C(2)	2660(10)	134(10)	-2671(10)	48(3)
C(3)	2099(9)	1428(10)	-1315(10)	47(3)
C(4)	51(10)	299(10)	-4401(9)	44(3)
C(5)	-1003(10)	1707(11)	-3484(9)	44(3)
C(6)	-231(8)	1463(8)	-1508(10)	34(3)
C(7)	-533(9)	-2251(9)	-1562(8)	32(2)
C(8)	-2119(10)	-641(11)	-284(8)	48(3)
C(9)	-2316(10)	432(11)	-434(9)	46(3)
C(10)	-1528(12)	968(10)	83(10)	51(4)
C(11)	-816(10)	293(11)	530(8)	48(3)
C(12)	-1176(11)	-726(11)	319(8)	46(3)
C(13)	1961(10)	-2158(10)	-3206(8)	39(3)
C(14)	1394(10)	-1698(11)	-3977(9)	44(3)
C(15)	356(12)	-2163(11)	-4106(9)	51(3)
C(16)	294(10)	-2939(11)	-3398(11)	54(4)
C(17)	1261(10)	-2938(9)	-2808(9)	40(3)

<sup>a</sup>  $U_{\text{eq}}$  is defined as one-third of the trace of the orthogonalized  $U_{ij}$  tensor.

Table 4  
Atomic coordinates ( $\times 10^4$ ) and equivalent isotropic displacement parameters ( $\text{\AA}^2 \times 10^3$ ) for 11

Atom	<i>x</i>	<i>y</i>	<i>z</i>	$U_{\text{eq}}^{\text{a}}$
Se(1)	0	2667(1)	2500	41(1)
Se(2)	0	-29(4)	1488(6)	31(1)
S(1)	0	226(10)	1554(15)	27(2)
Mo(2)	-1301(1)	1113(1)	2500	32(1)
Fe(1)	0	1734(1)	967(1)	35(1)
O(1)	0	3970(5)	528(5)	69(2)
O(2)	2101(5)	1327(4)	-236(3)	68(1)
C(1)	-3161(13)	129(12)	2500	117(7)
C(2)	-3218(7)	753(11)	1802(6)	113(5)
C(3)	-3263(6)	1757(8)	2058(6)	97(3)
C(4)	0	3120(7)	752(6)	45(2)
C(5)	1291(5)	1477(5)	251(4)	47(2)

<sup>a</sup>  $U_{\text{eq}}$  is defined as one-third of the trace of the orthogonalized  $U_{ij}$  tensor.

of benzene was refluxed for 24 h. The solution was filtered through Celite to remove insoluble material. After removal of the solvent from the filtrate, the residue was subjected to chromatographic work-up. Elution with hexane–dichloromethane (50/50 v/v) mixture yielded three fractions, each of which was subjected to further chromatographic work-up on silica gel TLC plates. Chromatography of the first fraction, using a hexane–dichloromethane (70/30 v/v) mixture as eluent, resulted in the following four compounds, in the order of elution: yellowish-brown  $\text{Cp}_2\text{Mo}_2\text{Fe}_2(\text{CO})_6\text{Te}_3$  (**1**; trace); deep yellowish-brown  $\text{Cp}_2\text{Mo}_2\text{Fe}_2(\text{CO})_6\text{SeTe}_2$  (**2**; 120 mg, 21%); brown  $\text{Cp}_2\text{Mo}_2\text{Fe}_2(\text{CO})_6\text{Se}_2\text{Te}$  (**3**); brown  $\text{Cp}_2\text{Mo}_2\text{Fe}_2(\text{CO})_6\text{Se}_3$  (**4**; trace). Repeated chromatography of compound **3** on high performance TLC plates, using a (1/99 v/v) THF–hexane mixture as eluent, separated the two isomers:  $\text{Cp}_2\text{Mo}_2\text{Fe}_2(\text{CO})_6(\mu_4\text{-Te})(\mu_3\text{-Se})_2$  (**3a**; 60 mg, 11%) and  $\text{Cp}_2\text{Mo}_2\text{Fe}_2(\text{CO})_6(\mu_4\text{-Se})(\mu_3\text{-Se})(\mu_3\text{-Te})$  (**3b**; 38 mg, 7%). Chromatography of the second fraction, using a hexane–dichloromethane (50/50 v/v) mixture as eluent, gave two dark red bands, in order of elution:  $\text{Cp}_2\text{Mo}_2\text{Fe}(\text{CO})_7\text{Te}$  (**5**; trace);  $\text{Cp}_2\text{Mo}_2\text{Fe}(\text{CO})_7\text{Se}$  (**6**; 44 mg, 11%). Chromatography of the third fraction, with a hexane–dichloromethane (40/60 v/v) mixture as eluent, separated the following three bands: black  $\text{Cp}_2\text{Mo}_2\text{Fe}_2(\text{CO})_7\text{Se}_2$  (**7**; 34 mg, 7%); dark brown  $\text{Cp}_2\text{Mo}_2\text{Fe}_2(\text{CO})_7\text{SeTe}$  (**8**; 117.3 mg, 23%); dark brown  $\text{Cp}_2\text{Mo}_2\text{Fe}_2(\text{CO})_7\text{Te}_2$  (**9**; 27 mg, 5%). **2**: m.p. 202–203 °C. Anal. Found: C, 20.6; H, 1.09.  $\text{C}_{16}\text{H}_{10}\text{Fe}_2\text{Mo}_2\text{O}_6\text{SeTe}_2$  calcd.: C, 20.5; H, 1.06%. **3a**: m.p. 143–144 °C. Anal. Found: C, 20.8; H, 1.23.  $\text{C}_{16}\text{H}_{10}\text{Fe}_2\text{Mo}_2\text{O}_6\text{Se}_2\text{Te}$  calcd.: C, 21.6; H, 1.12%. **3b**: m.p. 149–150 °C. Anal. Found: C, 21.2; H, 1.20.  $\text{C}_{16}\text{H}_{10}\text{Fe}_2\text{Mo}_2\text{O}_6\text{Se}_3$  calcd: C, 21.6; H, 1.12%. **8**: m.p. 126–127 °C (dec.). Anal. Found: C, 24.5; H, 1.31.  $\text{C}_{16}\text{H}_{10}\text{Fe}_2\text{Mo}_2\text{O}_7\text{SeTe}$  calcd.: C, 24.41; H, 1.22%.

### 2.3. Reaction of **8** with selenium powder

A benzene solution (50 ml) containing **8** (167 mg, 0.2 mmol) and selenium powder (23.7 mg, 0.3 mmol) was refluxed for 12 h. The reaction mixture was filtered through Celite to remove unreacted selenium powder, and the solvent was removed in vacuo. Repeated chromatography of the residue using a (1/99 v/v) THF–hexane mixture as eluent on high performance TLC

plates separated the two isomers of **3**,  $\text{Cp}_2\text{Mo}_2\text{Fe}_2(\text{CO})_6(\mu_4\text{-Te})(\mu_3\text{-Se})_2$  (**3a**; 94 mg, 53%) and  $\text{Cp}_2\text{Mo}_2\text{Fe}_2(\text{CO})_6(\mu_4\text{-Se})(\mu_3\text{-Se})(\mu_3\text{-Te})$  (**3b**; 34 mg, 19%), together with a trace amount of unreacted **8**.

### 2.4. Reaction of **9** with selenium powder

A benzene solution (50 ml) containing **9** (177 mg, 0.2 mmol) and selenium powder (23.7 mg, 0.3 mmol)

Table 5  
Selected bond lengths (Å) and bond angles (deg) for **3a**

Te(1)–Mo(2)	2.6021(14)	Te(2)–Fe(4)	2.720(2)
Te(1)–Mo(1)	2.6059(13)	Se(3)–Fe(3)	2.378(2)
Te(1)–Fe(1)	2.704(2)	Se(3)–Mo(3)	2.514(2)
Te(1)–Fe(2)	2.738(2)	Se(3)–Mo(4)	2.5376(14)
Se(1)–Fe(1)	2.349(2)	Se(4)–Fe(4)	2.352(2)
Se(1)–Mo(2)	2.5044(14)	Se(4)–Mo(3)	2.495(2)
Se(1)–Mo(1)	2.506(2)	Se(4)–Mo(4)	2.496(2)
Se(2)–Fe(2)	2.355(2)	Mo(2)–Fe(1)	2.893(2)
Se(2)–Mo(2)	2.498(2)	Mo(2)–Fe(2)	2.907(2)
Se(2)–Mo(1)	2.5056(14)	Mo(3)–Mo(4)	2.7554(13)
Te(2)–Mo(3)	2.6055(12)	Mo(3)–Fe(4)	2.895(2)
Te(2)–Mo(4)	2.6156(14)	Mo(3)–Fe(3)	2.911(2)
Te(2)–Fe(3)	2.718(2)		
Mo(2)–Te(1)–Mo(1)	63.94(4)	Mo(2)–Te(1)–Fe(1)	66.04(4)
Mo(2)–Te(1)–Fe(2)	65.90(5)	Mo(1)–Te(1)–Fe(2)	65.16(5)
Fe(1)–Te(1)–Fe(2)	122.17(5)	Fe(1)–Se(1)–Mo(2)	73.09(5)
Mo(2)–Se(1)–Mo(1)	66.78(4)	Fe(2)–Se(2)–Mo(2)	73.54(5)
Fe(2)–Se(2)–Mo(1)	72.59(5)	Mo(2)–Se(2)–Mo(1)	66.88(4)
Mo(3)–Te(2)–Mo(4)	63.71(4)	Mo(3)–Te(2)–Fe(3)	66.27(4)
Mo(4)–Te(2)–Fe(3)	64.72(5)	Mo(3)–Te(2)–Fe(4)	65.82(5)
Mo(4)–Te(2)–Fe(4)	65.49(5)	Fe(3)–Te(2)–Fe(4)	121.72(5)
Fe(3)–Se(3)–Mo(3)	72.99(5)	Fe(3)–Se(3)–Mo(4)	70.97(5)
Mo(3)–Se(3)–Mo(4)	66.11(4)	Fe(4)–Se(4)–Mo(3)	73.29(6)
Fe(4)–Se(4)–Mo(4)	73.05(6)	Mo(3)–Se(4)–Mo(4)	67.03(4)
Se(4)–Mo(4)–Se(3)	79.66(4)	Se(1)–Fe(1)–Te(1)	100.10(6)
Se(1)–Fe(1)–Mo(2)	55.93(5)	Te(1)–Fe(1)–Mo(2)	55.29(4)
Te(1)–Fe(1)–Mo(1)	55.36(4)	Mo(2)–Fe(1)–Mo(1)	56.91(4)
Se(2)–Fe(2)–Te(1)	99.55(6)	Se(2)–Mo(1)–Se(1)	80.12(5)
Se(2)–Mo(2)–Te(1)	99.60(5)	Se(1)–Mo(2)–Te(1)	98.88(4)
Se(2)–Mo(2)–Mo(1)	56.69(4)	Se(2)–Fe(2)–Mo(1)	56.13(4)
Te(1)–Fe(2)–Mo(1)	55.20(4)	Se(2)–Fe(2)–Mo(2)	55.50(5)
Te(1)–Fe(2)–Mo(2)	54.80(4)	Mo(1)–Fe(2)–Mo(2)	56.91(4)
Se(3)–Fe(3)–Te(2)	100.72(6)	Se(3)–Fe(3)–Mo(4)	57.13(4)
Te(2)–Fe(3)–Mo(4)	55.90(4)	Se(3)–Fe(3)–Mo(3)	55.66(5)
Te(2)–Fe(3)–Mo(3)	55.01(4)	Mo(4)–Fe(3)–Mo(3)	57.07(4)
Se(4)–Fe(4)–Te(2)	99.83(6)	Se(4)–Fe(4)–Mo(4)	55.77(5)
Te(2)–Fe(4)–Mo(4)	55.51(4)	Te(2)–Fe(4)–Mo(3)	55.19(4)
Mo(4)–Fe(4)–Mo(3)	56.91(4)	Se(1)–Mo(2)–Mo(1)	56.64(4)
Te(1)–Mo(2)–Mo(1)	58.10(3)	Se(2)–Mo(2)–Fe(1)	115.69(5)
Se(1)–Mo(2)–Fe(1)	50.98(4)	Te(1)–Mo(2)–Fe(1)	58.67(4)
Mo(1)–Mo(2)–Fe(1)	61.58(4)	Se(2)–Mo(2)–Fe(2)	50.97(5)
Se(1)–Mo(2)–Fe(2)	115.18(5)	Te(1)–Mo(2)–Fe(2)	59.30(4)
Mo(1)–Mo(2)–Fe(2)	61.04(4)	Fe(1)–Mo(2)–Fe(2)	110.44(5)
Se(4)–Mo(3)–Se(3)	80.14(5)	Se(4)–Mo(3)–Te(2)	99.31(5)
Se(3)–Mo(3)–Te(2)	100.28(4)	Se(4)–Mo(3)–Mo(4)	56.50(4)
Se(3)–Mo(3)–Mo(4)	57.36(4)	Te(2)–Mo(3)–Mo(4)	58.32(3)
Se(4)–Mo(3)–Fe(4)	51.09(5)	Se(3)–Mo(3)–Fe(4)	116.04(5)
Te(2)–Mo(3)–Fe(4)	58.99(4)	Mo(4)–Mo(3)–Fe(4)	61.40(5)
Se(4)–Mo(3)–Fe(3)	114.46(5)	Se(3)–Mo(3)–Fe(3)	51.35(5)
Te(2)–Mo(3)–Fe(3)	58.72(4)	Mo(4)–Mo(3)–Fe(3)	60.46(4)
Fe(4)–Mo(3)–Fe(3)	109.76(5)		

Table 6  
Selected bond lengths ( $\text{\AA}$ ) and bond angles (deg) for **8**

Mo(1)–Se(1)	2.609(9)	Mo(2)–Te(1)	2.612(4)
Mo(1)–Te(1)	2.624(4)	Mo(2)–Fe(2)	2.840(2)
Mo(1)–Fe(1)	2.830(2)	Se(1)–Fe(1)	2.378(9)
Mo(1)–Fe(2)	2.833(2)	Te(1)–Fe(2)	2.408(3)
Mo(2)–Se(1)	2.627(11)	Fe(1)–Fe(2)	2.438(2)
Se(1)–Mo(2)–Te(1)	113.9(2)	Fe(2)–Fe(1)–Mo(1)	64.57(5)
Se(1)–Mo(2)–Fe(2)	95.3(2)	Fe(2)–Fe(1)–Mo(2)	64.36(5)
Te(1)–Mo(2)–Fe(2)	52.23(6)	Mo(1)–Fe(1)–Mo(2)	60.21(4)
Se(1)–Mo(2)–Mo(1)	56.7(2)	Te(1)–Fe(2)–Fe(1)	114.05(12)
Te(1)–Mo(2)–Mo(1)	57.21(8)	Se(1)–Mo(1)–Fe(1)	51.7(2)
Fe(2)–Mo(2)–Mo(1)	59.71(4)	Te(1)–Mo(1)–Fe(1)	96.34(9)
Fe(1)–Se(1)–Mo(1)	69.0(2)	Se(1)–Mo(1)–Fe(2)	95.8(2)
Fe(1)–Se(1)–Mo(2)	69.3(3)	Te(1)–Mo(1)–Fe(2)	52.21(8)
Mo(1)–Se(1)–Mo(2)	66.0(2)	Fe(1)–Mo(1)–Fe(2)	51.01(4)
Fe(2)–Te(1)–Mo(1)	68.37(8)	Te(1)–Fe(2)–Mo(1)	59.42(10)
Fe(2)–Te(1)–Mo(2)	68.77(11)	Fe(1)–Fe(2)–Mo(1)	64.42(5)
Mo(1)–Te(1)–Mo(2)	65.98(9)	Fe(1)–Fe(2)–Mo(2)	64.93(5)
Se(1)–Mo(1)–Te(1)	114.1(2)	Te(1)–Fe(2)–Mo(2)	59.00(10)
Se(1)–Fe(1)–Fe(2)	114.1(3)	Mo(1)–Fe(2)–Mo(2)	60.33(4)
Se(1)–Fe(1)–Mo(1)	59.4(2)		

was refluxed for 12 h. The reaction mixture was filtered through Celite to remove unreacted selenium powder, and solvent was removed from the filtrate. Chromatographic work-up of the residue on silica gel TLC plates with a hexane–dichloromethane (70/30 v/v) mixture yielded a single major product, a yellowish brown band of **2** (95 mg, 51%) followed by a trace of unreacted **9**.

#### 2.5. Thermolytic reaction of $\text{Fe}_3(\text{CO})_9\text{SSe}$ with $\text{Cp}_2\text{Mo}_2(\text{CO})_6$

A mixture of  $\text{Fe}_3(\text{CO})_9(\mu_3\text{-S})(\mu_3\text{-Se})$ , (0.47 g, 0.88 mmol) and  $\text{Cp}_2\text{Mo}_2(\text{CO})_6$  (0.3 g, 0.61 mmol) in 100 ml of benzene was refluxed for 24 h. The solvent

was removed in vacuo and the residue was subjected to chromatographic work-up. Using a hexane–dichloromethane (50/50 v/v) mixture as eluent, three fractions were collected, each of which was subjected to further chromatographic work-up on silica gel TLC plates. Chromatographic work-up of the first fraction, using a hexane–dichloromethane (70/30 v/v) mixture as eluent, yielded three compounds: yellowish-brown  $\text{Cp}_2\text{Mo}_2\text{Fe}_2(\text{CO})_6\text{S}_2\text{Se}$  (**10**; trace); brown  $\text{Cp}_2\text{Mo}_2\text{Fe}_2(\text{CO})_6\text{SSe}_2$  (**11**; 92 mg, 19%); brown  $\text{Cp}_2\text{Mo}_2\text{Fe}_2(\text{CO})_6\text{Se}_3$  (4; trace). Chromatography of the second fraction, with a hexane–dichloromethane (50/50 v/v) mixture as eluent, gave two dark red bands:  $\text{Cp}_2\text{Mo}_2\text{Fe}(\text{CO})_7\text{Se}$  (**6**; trace) and  $\text{Cp}_2\text{Mo}_2\text{Fe}(\text{CO})_7\text{S}$  (**12**; trace). Chromatography of the third fraction, using a hexane–dichloromethane (40/60 v/v) mixture as eluent, afforded two products, in the order of elution: dark brown  $\text{Cp}_2\text{Mo}_2\text{Fe}_2(\text{CO})_7\text{SSe}$  (**13**; 95 mg, 21%) and brown  $\text{Cp}_2\text{Mo}_2\text{Fe}_2(\text{CO})_7\text{Se}_2$  (**7**; 63 mg, 13%). **10**: m.p. 120–122 °C (dec.). Anal. Found: C, 25.7; H, 1.43.  $\text{C}_{16}\text{H}_{10}\text{Fe}_2\text{Mo}_2\text{O}_6\text{S}_2\text{Se}$  calcd.: C, 25.8; H, 1.34%. **11**: m.p. 121–122 °C (dec.). Anal. Found: C, 24.3; H, 1.4.  $\text{C}_{16}\text{H}_{10}\text{Fe}_2\text{Mo}_2\text{O}_6\text{SSe}_2$  calcd.: C, 24.2; H, 1.26%. **13**: m.p. 154–155 °C (dec.). Anal. Found: C, 27.4; H, 1.46.  $\text{C}_{17}\text{H}_{10}\text{Fe}_2\text{Mo}_2\text{O}_7\text{SSe}$  calcd.: C, 27.3; H, 1.35%.

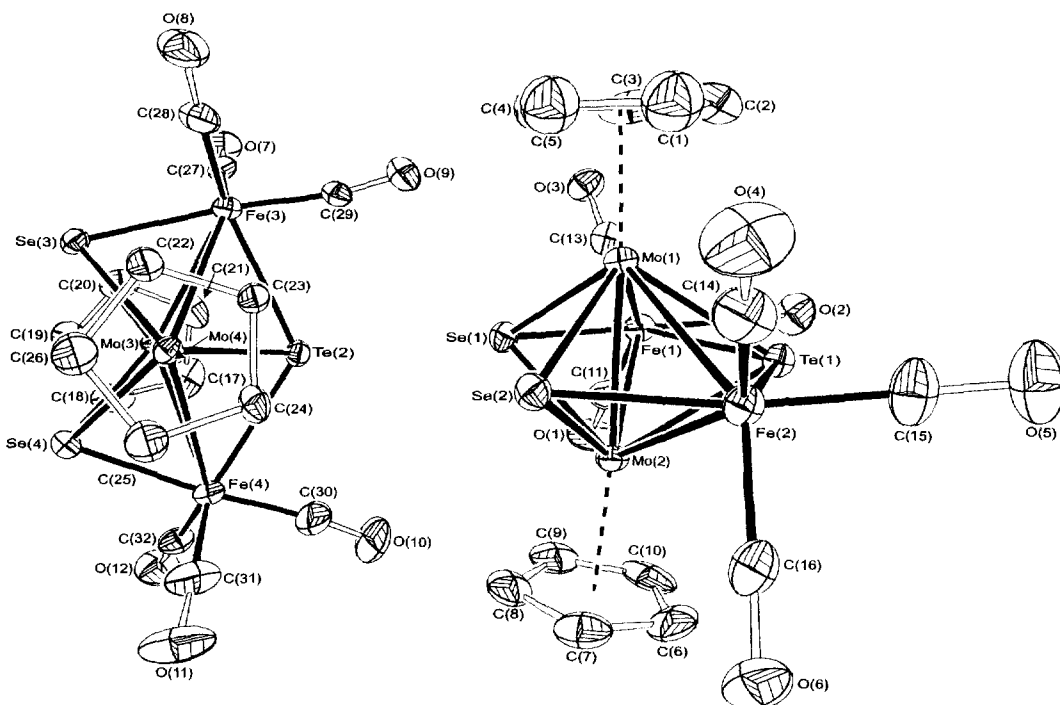
#### 2.6. Reaction of **7** with sulphur powder

A benzene solution (50 ml) containing **7** (158 mg, 0.2 mmol) and sulphur powder (13 mg, 0.4 mmol) was refluxed for 3 h. The reaction mixture was filtered through Celite to remove unreacted sulphur powder. Solvent was removed in vacuo. Chromatographic work-up of the residue on silica gel TLC plates with a hexane–dichloromethane (70/30 v/v) mixture gave as

Table 7  
Selected bond lengths ( $\text{\AA}$ ) and bond angles (deg) for **11**

Se(1)–Mo(2)	2.4068(10)	S(1)–Fe(1)	2.13(2)
Se(1)–Fe(1)	2.6437(11)	S(1)–Mo(2)	2.292(13)
Se(2)–Fe(1)	2.390(7)	Mo(2)–Fe(1) <sup>b</sup>	2.8363(10)
Se(2)–Mo(2)	2.531(5)	Mo(2)–Mo(2) <sup>a</sup>	2.7194(12)
Mo(2)–Se(1)–Mo(2) <sup>a</sup>	68.80(4)	Mo(2)–Se(1)–Fe(1) <sup>a</sup>	68.14(3)
Fe(1)–Se(1)–Fe(1) <sup>b</sup>	126.36(6)	Fe(1)–Se(2)–Mo(2)	70.33(11)
Mo(2) <sup>a</sup> –Se(2)–Mo(2)	65.00(14)	Fe(1)–S(1)–Mo(2)	79.8(3)
Mo(2) <sup>a</sup> –S(1)–Mo(2)	72.85(5)	S(1)–Mo(2)–S(1) <sup>b</sup>	78.9(10)
S(1)–Mo(2)–Se(1)	94.23(3)	S(1)–Mo(2)–Se(2)	5.8(4)
S(1) <sup>b</sup> –Mo(2)–Se(2)	77.7(3)	Se(1)–Mo(2)–Se(2)	99.91(10)
Se(2)–Mo(2)–Se(2) <sup>b</sup>	76.0(4)	S(1)–Mo(2)–Mo(2) <sup>a</sup>	53.6(2)
Se(2)–Mo(2)–Mo(2) <sup>a</sup>	57.50(7)	S(1)–Mo(2)–Fe(1) <sup>b</sup>	112.5(3)
S(1) <sup>b</sup> –Mo(2)–Fe(1) <sup>b</sup>	47.6(5)	Se(1)–Mo(2)–Fe(1) <sup>b</sup>	59.89(2)
Se(2)–Mo(2)–Fe(1) <sup>b</sup>	114.57(13)	Se(2) <sup>b</sup> –Mo(2)–Fe(1) <sup>b</sup>	52.5(2)
Mo(2) <sup>a</sup> –Mo(2)–Fe(1) <sup>b</sup>	61.35(2)	S(1)–Fe(1)–Se(2)	5.5(7)
S(1)–Fe(1)–Se(1)	91.7(5)	Se(2)–Fe(1)–Se(1)	97.2(2)
S(1)–Fe(1)–Mo(2)	52.7(4)	Se(2)–Fe(1)–Mo(2)	57.2(2)
Se(1)–Fe(1)–Mo(2)	51.96(3)	Mo(2) <sup>a</sup> –Fe(1)–Mo(2)	57.29(3)

Symmetry transformations used to generate equivalent atoms: <sup>a</sup>  $-x, y, -z + 1/2$ ; <sup>b</sup>  $x, y, -z + 1/2$ ; <sup>c</sup>  $-x, y, z$ .

Fig. 1. Molecular structure of  $\text{Cp}_2\text{Mo}_2\text{Fe}_2(\text{CO})_6(\mu_3\text{-Se})_2(\mu_4\text{-Te})$  (**3a**).

the major product a yellowish-brown band of **11** (128 mg, 81%) and a trace amount of unreacted **7**.

#### 2.7. Reaction of **13** with sulphur powder

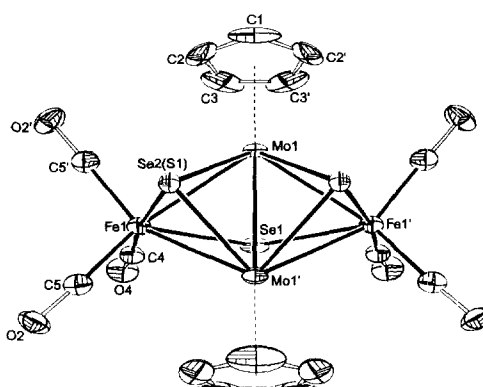
A benzene solution (30 ml) containing **13** (22 mg, 0.03 mmol) and sulphur powder (2 mg, 0.06 mmol) was refluxed for 3 h. The reaction mixture was filtered through Celite to remove unreacted sulphur powder. Solvent was removed in vacuo. Chromatographic work-up of the residue on silica gel TLC plates, with a hexane–dichloromethane (85/15 v/v) mixture, separated the yellowish-brown band of **10** (9 mg, 41%) from a trace amount of unreacted **13**.

#### 2.8. Crystal structure determination of **3a**, **8** and **11**

Crystals of compounds **3a**, **8** and **11** suitable for X-ray diffraction analysis were grown from hexane and dichloromethane solvent mixtures by slow evaporation of the solvents at 0 °C. Relevant crystallographic data and details of measurement are given in Table 1. Atomic coordinates and equivalent isotropic displacement parameters for **3a**, **8** and **11** are given in Tables 2–4 respectively. Selected bond lengths and bond angles for **3a**, **8** and **11** are given in Tables 5–7 respectively. Crystallographic data were measured at 293(2) K on a CAD4 automatic four circle diffractometer. Data were corrected for Lorentz and polarisation and also for absorption [13]. In the final least squares cycles all atoms were allowed to vibrate anisotropically. Hydro-

gen atoms were included at calculated positions where relevant. The solutions of the structures were carried out using SHELXS-86 [14] and the refinements were performed using SHELXL-93 [15]. The asymmetric units (shown in Figs. 1–3) along with the labelling scheme used were produced using ORTEP [16].

The asymmetric unit in compound **3a** was seen to consist of two molecules with one Cp ring in each molecule being disordered. In particular, the Cp ring containing C(1)–C(5) was disordered with the ring containing C(1A)–C(5A) in the ratio 54:46. Similarly, the Cp ring containing C(22)–C(26) was disordered with the ring containing C(22A)–C(26A) in the ratio 48:52. These partial occupancy rings were refined as rigid pentagons. Careful analysis of the structural refinement

Fig. 2. Molecular structure of  $\text{Cp}_2\text{Mo}_2\text{Fe}_2(\text{CO})_6(\mu_3\text{-S})(\mu_3\text{-Se})_4(\mu_4\text{-Se})$  (**11**).

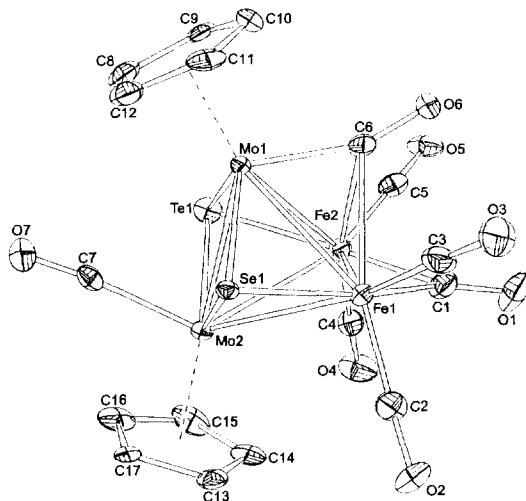


Fig. 3. Molecular structure of  $\text{Cp}_2\text{Mo}_2\text{Fe}_2(\text{CO})_7(\mu_3\text{-Se})(\mu_3\text{-Te})$  (8).

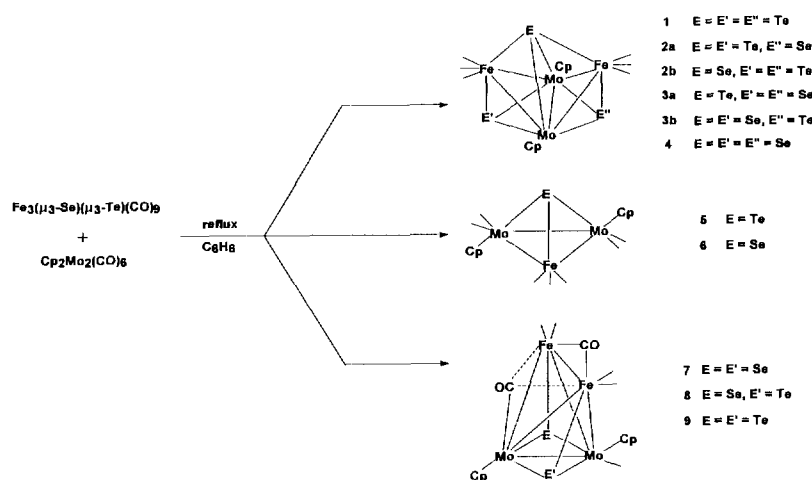
did not indicate any chalcogen disorder. In compound **8** the selenium and the tellurium atoms (Se(1) and Te(1)) exhibited disorder in the ratio 64:36 with their primed counterparts. Only the former are illustrated in the ORTEP plot, for clarity. For compound **11** the asymmetric unit actually consists of 1/4 of a molecule, as a result of space group and molecular symmetry. Typically, the molecule as presented possesses two mutually perpendicular mirror planes, with Mo(1) and C(1) sitting on a vertical plane, and Fe(1), Se(2)/S(1), C(4) and O(1) placed on a horizontal plane and Se(1) with the highest site-symmetry possible for space group *Cmcm*, namely *m2m*. The S(1)/Se(2) positions are consequently disordered in the ratio 1:1 (only the Se(2) position is illustrated in the plot for clarity).

### 3. Results and discussion

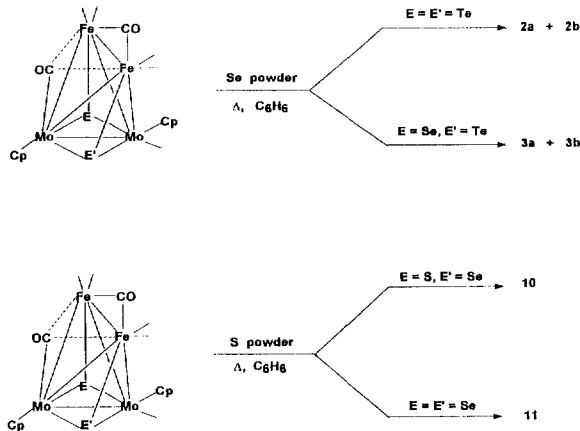
#### 3.1. Synthesis

When a benzene solution containing  $\text{Fe}_3(\text{CO})_9(\mu_3\text{-Se})(\mu_3\text{-Te})$  and  $\text{Cp}_2\text{Mo}_2(\text{CO})_6$  was refluxed for 24 h, the following clusters were obtained (Scheme 1):  $\text{Cp}_2\text{Mo}_2\text{Fe}_2(\text{CO})_6\text{Te}_3$  (**1**; trace);  $\text{Cp}_2\text{Mo}_2\text{Fe}_2(\text{CO})_6\text{SeTe}_2$  (**2**; 21%);  $\text{Cp}_2\text{Mo}_2\text{Fe}_2(\text{CO})_6\text{Se}_2\text{Te}$  (**3**);  $\text{Cp}_2\text{Mo}_2\text{Fe}_2(\text{CO})_6\text{Se}_3$  (**4**; trace);  $\text{Cp}_2\text{Mo}_2\text{Fe}(\text{CO})_7\text{Te}$  (**5**; trace);  $\text{Cp}_2\text{Mo}_2\text{Fe}(\text{CO})_7\text{Se}$  (**6**; 11%);  $\text{Cp}_2\text{Mo}_2\text{Fe}_2(\text{CO})_7\text{Se}_2$  (**7**; 7%);  $\text{Cp}_2\text{Mo}_2\text{Fe}_2(\text{CO})_7\text{SeTe}$  (**8**; 23%);  $\text{Cp}_2\text{Mo}_2\text{Fe}_2(\text{CO})_7\text{Te}_2$  (**9**; 5%). Repeated chromatography of **3** on TLC plates separated its two isomers,  $\text{Cp}_2\text{Mo}_2\text{Fe}_2(\text{CO})_6(\mu_4\text{-Te})(\mu_3\text{-Se})_2$  (**3a**; 60 mg, 11%) and  $\text{Cp}_2\text{Mo}_2\text{Fe}_2(\text{CO})_6(\mu_4\text{-Se})(\mu_3\text{-Se})(\mu_3\text{-Te})$  (**3b**; 38 mg, 7%). Attempts to obtain a separation of two isomers of **2** were unsuccessful. However, NMR spectroscopy confirmed that two isomers of **2**,  $\text{Cp}_2\text{Mo}_2\text{Fe}_2(\text{CO})_6(\mu_3\text{-Te})(\mu_3\text{-Se})(\mu_4\text{-Te})$  (**2a**) and  $\text{Cp}_2\text{Mo}_2\text{Fe}_2(\text{CO})_6(\mu_3\text{-Te})_2(\mu_4\text{-Se})$  (**2b**) were formed in the reaction (vide infra). Of these clusters, compounds **2a**, **2b**, **3a**, **3b** and **8** are new. Compounds **3a** and **3b** were isolated in better yields, 53% and 19% respectively, when a benzene solution of **8** and selenium powder was refluxed for 12 h (Scheme 2). Similarly, cluster **2** could be obtained in 51% yield when a benzene solution of **9** and selenium powder was refluxed for 12 h.

When a benzene solution containing  $\text{Fe}_3(\text{CO})_9(\mu_3\text{-S})(\mu_3\text{-Se})$  and  $\text{Cp}_2\text{Mo}_2(\text{CO})_6$  was refluxed for 24 h, the following new S/Se clusters were obtained (Scheme 3):  $\text{Cp}_2\text{Mo}_2\text{Fe}_2(\text{CO})_6\text{S}_2\text{Se}$  (**10**; trace);  $\text{Cp}_2\text{Mo}_2\text{Fe}_2(\text{CO})_6\text{SSe}_2$  (**11**; 19%);



Scheme 1.



Scheme 2.

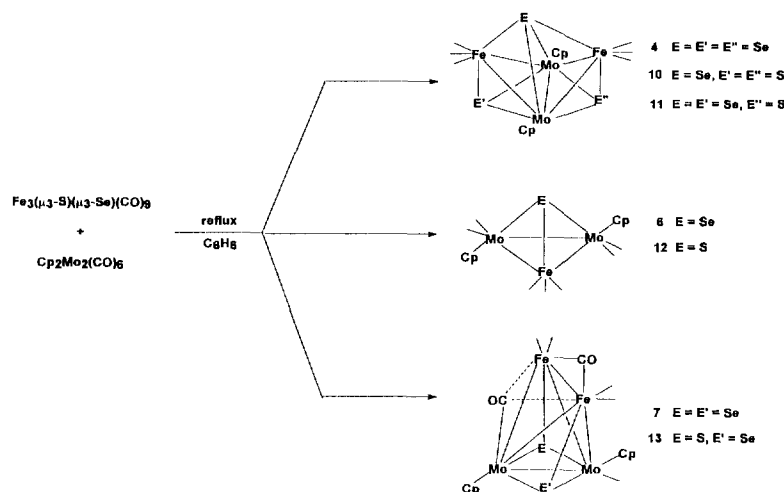
$\text{Cp}_2\text{Mo}_2\text{Fe}_2(\text{CO})_7\text{SSe}$  (**13**; 21%). Also obtained from the reaction were  $\text{Cp}_2\text{Mo}_2\text{Fe}_2(\text{CO})_6\text{Se}_3$  (**4**; trace),  $\text{Cp}_2\text{Mo}_2\text{Fe}(\text{CO})_7\text{Se}$  (**6**; trace),  $\text{Cp}_2\text{Mo}_2\text{Fe}(\text{CO})_7\text{S}$  (**12**; trace) and  $\text{Cp}_2\text{Mo}_2\text{Fe}_2(\text{CO})_7\text{Se}_2$  (**7**; 13%). An improved yield of **10** (41%) could be obtained when a benzene solution of **13** and sulphur powder was refluxed for 3 h. Similarly, refluxing of benzene solutions of **7** and sulphur powder produced  $\text{Cp}_2\text{Mo}_2\text{Fe}_2(\text{CO})_6\text{SSe}_2$  (**11**; 81%). Even after repeated chromatography we could not observe those isomers of **10** and **11** in which the  $\mu_4$ -sites were occupied by the S ligand.  $^{77}\text{Se}$  NMR spectroscopy of **10** and **11** also showed the presence of only one isomer in each case (vide infra).

### 3.2. Spectroscopic characterisation

The new trichalcogenide clusters **2a**, **2b**, **3a**, **3b**, **10** and **11** and the new dichalcogenide clusters **8** and **13** were characterised by IR and  $^1\text{H}$ ,  $^{13}\text{C}$ ,  $^{77}\text{Se}$ ,  $^{125}\text{Te}$  NMR

spectroscopy (Table 8). All other compounds were identified on the basis of comparison of their IR spectra in the carbonyl stretching region with those reported earlier [7,8]. The IR spectra of **2**, **3a**, **3b**, **10** and **11** indicate the presence of terminally bonded carbonyl groups, typically in the range of 1940 to 2028  $\text{cm}^{-1}$ . There is a regular decrease in the carbonyl stretching frequencies of the corresponding bands along the following series of chalcogen combinations:  $\text{S}_2\text{Se}$ ,  $\text{SSe}_2$ ,  $\text{Se}_2\text{Te}$ ,  $\text{SeTe}_2$ . The  $^1\text{H}$  NMR spectra of the trichalcogenide clusters **2**, **3a**, **3b**, **10** and **11** each show a single peak for the two equivalent Cp ligands. The  $^{13}\text{C}$  NMR spectra for the trichalcogenide compounds show a single peak for the CO ligands, indicating that at room temperature all carbonyl groups are equivalent on the NMR time scale. The  $^{125}\text{Te}$  NMR spectroscopy has been useful for differentiating between triply bridging and quadruply bridging Te atoms, the signal for the former appearing more upfield ( $\delta = 705$  to 721 ppm) in contrast to that for the  $\mu_4$ -Te, where  $\delta > 1600$  ppm downfield with respect to  $\text{Te}(\text{CH}_3)_2$  [8]. For compound **2**, the  $^{125}\text{Te}$  NMR signal shows the presence of two signals, at  $\delta$  721 ppm and at  $\delta$  1688 ppm indicating the presence of triply bridging as well as quadruply bridging Te atoms. In case of **3a**, there is only one  $^{125}\text{Te}$  NMR signal ( $\delta$  1683 ppm), due to a  $\mu_4$ -Te ligand. The  $^{125}\text{Te}$  NMR spectrum for compound **3b**, on the other hand, shows a highfield peak ( $\delta$  705 ppm) which can be attributed to a  $\mu_3$ -Te ligand, indicating that in **3b** it is the lighter Se atom which occupies the quadruply bridging mode.

$^{77}\text{Se}$  NMR spectroscopy can be used to distinguish between the triply and the quadruply bonded Se atoms; the signal for the former appears in the range  $\delta$  650–680 ppm and the signal for the  $\mu_4$ -Se ligands appear at  $\delta$  1280–1340 ppm. The  $^{77}\text{Se}$  NMR spectrum of **2** shows



Scheme 3.

Table 8  
Spectroscopic data for compounds **2a/2b**, **3a**, **3b**, **8**, **10**, **11**, **13**

Compounds	IR ( $\nu$ , $\text{cm}^{-1}$ )	$^1\text{H}$ NMR ( $\delta$ , $\text{CDCl}_3$ )	$^{13}\text{C}$ NMR ( $\delta$ , $\text{CDCl}_3$ )	$^{77}\text{Se}$ NMR ( $\delta$ , $\text{CDCl}_3$ )	$^{125}\text{Te}$ NMR ( $\delta$ , $\text{CDCl}_3$ )
$\text{Cp}_2\text{Mo}_2\text{Fe}_2\text{SeTe}_2(\text{CO})_6$ ( <b>2a/2b</b> )	2014(w) <sup>a</sup> , 1995(vs), 1953(m,br), 1942(m)	4.75 ( $\text{C}_5\text{H}_5$ )	87 ( $\text{C}_5\text{H}_5$ ) 213 (CO)	659 ( $\mu_3\text{-Se}$ ) 1327 ( $\mu_4\text{-Se}$ )	721 ( $\mu_3\text{-Te}$ ) 1688 ( $\mu_4\text{-Te}$ )
$\text{Cp}_2\text{Mo}_2\text{Fe}_2\text{Se}_2\text{Te}(\text{CO})_6$ ( <b>3a</b> )	2018(w) <sup>a</sup> , 1999(vs), 1957(m), 1943(m)	4.86 ( $\text{C}_5\text{H}_5$ )	89 ( $\text{C}_5\text{H}_5$ ) 213 (CO)	663.64 ( $\mu_3\text{-Se}$ )	1683 ( $\mu_4\text{-Te}$ )
$\text{Cp}_2\text{Mo}_2\text{Fe}_2\text{Se}_2\text{Te}(\text{CO})_6$ ( <b>3b</b> )	2018(w) <sup>a</sup> , 1999(vs), 1957(m), 1943(m)	4.90 ( $\text{C}_5\text{H}_5$ )	89 ( $\text{C}_5\text{H}_5$ ) 213 (CO)	663.84 ( $\mu_3\text{-Se}$ ) 1338 ( $\mu_4\text{-Se}$ )	705 ( $\mu_3\text{-Te}$ )
$\text{Cp}_2\text{Mo}_2\text{Fe}_2\text{SeTe}(\text{CO})_7$ ( <b>8</b> )	2015(vs) <sup>b</sup> , 1988(vs), 1955(s), 1825(m,br), 1734(w)	5.13 ( $\text{C}_5\text{H}_5$ ) 5.44 ( $\text{C}_5\text{H}_5$ )	91 ( $\text{C}_5\text{H}_5$ ) 93 ( $\text{C}_5\text{H}_5$ ) 198 (CO) 209 (CO)	1098 ( $\mu_3\text{-Se}$ )	1333 ( $\mu_3\text{-Te}$ )
$\text{Cp}_2\text{Mo}_2\text{Fe}_2\text{S}_2\text{Se}(\text{CO})_6$ ( <b>10</b> )	2028(vs) <sup>a</sup> , 2006(vs), 1958(m,br), 1809(w)	5.17 ( $\text{C}_3\text{H}_5$ )	94 ( $\text{C}_5\text{H}_5$ ) 213 (CO)	1283 ( $\mu_4\text{-Se}$ )	—
$\text{Cp}_2\text{Mo}_2\text{Fe}_2\text{Se}_2\text{S}(\text{CO})_6$ ( <b>11</b> )	2024(w) <sup>a</sup> , 2005(vs), 1957(m,br)	5.09 ( $\text{C}_5\text{H}_5$ )	93 ( $\text{C}_5\text{H}_5$ ) 213 (CO)	680 ( $\mu_3\text{-Se}$ ) 1310 ( $\mu_4\text{-Se}$ )	—
$\text{Cp}_2\text{Mo}_2\text{Fe}_2\text{SSe}(\text{CO})_7$ ( <b>13</b> )	2019(m) <sup>b</sup> , 1990(vs), 1956(w), 1832(m,br), 1740(sh)	5.21 ( $\text{C}_5\text{H}_5$ ) 5.54 ( $\text{C}_5\text{H}_5$ )	92 ( $\text{C}_5\text{H}_5$ ) 95 ( $\text{C}_5\text{H}_5$ ) 211 (CO) 213 (CO)	1051 ( $\mu_3\text{-Se}$ )	—

<sup>a</sup> Hexane.

<sup>b</sup>  $\text{CH}_2\text{Cl}_2$ .

two signals, one corresponding to the  $\mu_3\text{-Se}$  atom ( $\delta$  659 ppm) and the other to the  $\mu_4\text{-Se}$  atom ( $\delta$  1327 ppm). The existence of two isomers for compound **3** is also confirmed by  $^{77}\text{Se}$  NMR data. In the case of  $\text{Cp}_2\text{Mo}_2\text{Fe}_2(\text{CO})_6(\mu_4\text{-Te})(\mu_3\text{-Se})_2$  (**3a**), a single peak is observed at  $\delta$  663.6 ppm for the  $\mu_3\text{-Se}$  atoms. For  $\text{Cp}_2\text{Mo}_2\text{Fe}_2(\text{CO})_6(\mu_4\text{-Se})(\mu_3\text{-Te})(\mu_3\text{-Se})$  (**3b**) we observe two signals, one at  $\delta$  663.8 ppm due to the  $\mu_3\text{-Se}$  atom and another at  $\delta$  1338 ppm due to the  $\mu_4\text{-Se}$  ligand. For compound **10**, there is only one peak ( $\delta$  1283 ppm) corresponding to a  $\mu_4\text{-Se}$  atom, and for **11** the  $^{77}\text{Se}$  NMR shows two signals, one at  $\delta$  680 ppm due to a  $\mu_3\text{-Se}$  atom and the other at  $\delta$  1310 ppm due to a  $\mu_4\text{-Se}$  atom. In both these compounds the formation of isomers with a quadruply bridging S atom was not observed.

The IR spectra of the dichalcogenide clusters **8** and **13** display carbonyl stretching frequencies in the range 1734–2019  $\text{cm}^{-1}$  indicating the presence of bridging as well as terminal carbonyl groups. The CO stretching pattern is similar to that observed for the previously reported  $\text{Cp}_2\text{Mo}_2\text{Fe}_2(\text{CO})_7(\mu_3\text{-Te})(\mu_3\text{-E})$ , (E = S, Te) [8] and  $\text{Cp}_2\text{Mo}_2\text{Fe}_2(\text{CO})_7(\mu_3\text{-Se})_2$  [7], which contain terminal, doubly bridging and semitriply bridging carbonyl ligands. The dichalcogenide clusters **8** and **13** show two  $^1\text{H}$  NMR signals due to the two non-equivalent Cp groups. A variable-temperature NMR study of the dichalcogenide systems in toluene medium confirmed the non-equivalence of the two Cp ligands at up to 100 °C. The  $^{77}\text{Se}$  NMR spectrum for **8** shows a single

peak, 26 ppm downfield of that observed for the previously reported  $\text{Cp}_2\text{Mo}_2\text{Fe}_2(\text{CO})_7(\mu_3\text{-Se})_2$ . The spectrum of **13** shows a peak which is 20 ppm upfield of that of  $\text{Cp}_2\text{Mo}_2\text{Fe}_2(\text{CO})_7(\mu_3\text{-Se})_2$ . Comparison of the  $^{77}\text{Se}$  NMR spectra of the mixed-metal dichalcogenide clusters  $\text{Cp}_2\text{Mo}_2\text{Fe}_2(\text{CO})_7(\mu_3\text{-Se})(\mu_3\text{-E})$  shows a regular downfield shift of the signal along the series E = S, Se, Te. A similar trend is also observed in the  $^{125}\text{Te}$  NMR chemical shifts of the mixed-metal dichalcogenides:  $\text{Cp}_2\text{Mo}_2\text{Fe}_2(\text{CO})_7(\mu_3\text{-S})(\mu_3\text{-Te})$  ( $\delta$  1293 ppm), **8** ( $\delta$  1333 ppm) and  $\text{Cp}_2\text{Mo}_2\text{Fe}_2(\text{CO})_7(\mu_3\text{-Te})_2$  ( $\delta$  1386 ppm).

### 3.3. Molecular structures

The molecular structures of **3a** and **11** are depicted in Figs. 1 and 2 respectively. The two clusters have an identical heavy atom skeleton consisting of an  $\text{Mo}_2\text{Fe}_2$  butterfly arrangement. The Mo atoms occupy the hinge-sites and the Fe atoms are located at the wing tips. In **3a**, the four metal atoms are bridged by a  $\mu_4\text{-Te}$  atom and in **11** by a  $\mu_4\text{-Se}$  atom. The two  $\text{Mo}_2\text{Fe}$  faces in **3a** are capped by a  $\mu_3\text{-Se}$  atom each and in **11** by a  $\mu_3\text{-S}$  and a  $\mu_3\text{-Se}$  atom. Each Mo atom has an ( $\eta^5\text{-C}_5\text{H}_5$ ) group attached to it and each Fe atom has three terminally bonded carbonyl groups. The structures are similar to those of the previously reported  $\text{Cp}_2\text{Mo}_2\text{Fe}_2(\text{CO})_6(\mu_3\text{-E})(\mu_3\text{-E'})(\mu_4\text{-Te})$  (E,E' = Te,Te; S,Te; S,S and S,Se) [8] and  $\text{Cp}_2\text{Mo}_2\text{Fe}_2(\text{CO})_6(\mu_3\text{-Se})_2(\mu_4\text{-Se})$  [7]. In **3a** the Mo-

Mo bond distance ( $2.7554(13)\text{ \AA}$ ) is slightly longer than the Mo–Mo bond distance of **11** ( $2.7194(12)\text{ \AA}$ ). The average Mo–Fe bond distance in **3a** ( $2.902\text{ \AA}$ ) is also longer than the average Mo–Fe bond distance in **11** ( $2.836\text{ \AA}$ ). A similar trend of metal–metal bond length dependence on the size of the chalcogen ligands bridging the butterfly-core of metal atoms in such clusters has been previously noted [8].

The molecular structure of **8** is shown in Fig. 3. It consists of an  $\text{Mo}_2\text{Fe}_2$  tetrahedron with one  $\text{Mo}_2\text{Fe}$  face capped by a  $\mu_3\text{-Te}$  atom and the other by a  $\mu_3\text{-S}$  atom. One Mo atom possesses a semitriply bridging CO ligand ( $\text{Mo}(1)\text{-C}(6)\text{-O}(6)$ ,  $157.9(10)^\circ$ ). There are two terminally bonded carbonyl ligands on each Fe atom and one carbonyl group bridges the Fe–Fe bond. Each Mo atom has an  $\eta^5\text{-C}_5\text{H}_5$  group and the unbridged Mo atom has a terminal carbonyl group oriented away from the cluster core. Overall, the structure is similar to the previously reported  $\text{Cp}_2\text{Mo}_2\text{Fe}_2(\text{CO})_7(\mu_3\text{-Te})_2$  [17],  $\text{Cp}_2\text{Mo}_2\text{Fe}_2(\text{CO})_7(\mu_3\text{-Se})_2$  and  $\text{Cp}_2\text{Mo}_2\text{Fe}_2(\text{CO})_7(\mu_3\text{-S})(\mu_3\text{-Te})$  [8] structures. The Fe–Fe bond distance in **8** ( $2.438(2)\text{ \AA}$ ) is shorter than that in  $\text{Cp}_2\text{Mo}_2\text{Fe}_2(\text{CO})_7(\mu_3\text{-S})(\mu_3\text{-Te})$  ( $2.545(2)\text{ \AA}$ ), but similar to those in  $\text{Cp}_2\text{Mo}_2\text{Fe}_2(\text{CO})_7(\mu_3\text{-Te})_2$  ( $2.433(2)\text{ \AA}$ ) and  $\text{Cp}_2\text{Mo}_2\text{Fe}_2(\text{CO})_7(\mu_3\text{-Se})_2$  ( $2.442(2)\text{ \AA}$ ). Other bond metricals are unexceptional.

#### 4. Conclusion

It is now possible to make certain general observations from a study of these reactions. They can be summarised as follows. It has been observed that the sulphur-containing trinuclear cluster  $\text{Fe}_3(\text{CO})_9(\mu_3\text{-S})_2$  on thermolysis with  $\text{Cp}_2\text{Mo}_2(\text{CO})_6$  in benzene solution does not form the mixed-metal trichalcogenide or dichalcogenide compounds, although when sulphur is present in a trinuclear starting material in combination with either selenium or tellurium the mixed-metal trichalcogenide and dichalcogenide compounds are formed readily. The yields of the mixed-metal trichalcogenide and dichalcogenide compounds are much higher in the case of the trinuclear heterochalcogenide systems than for the homochalcogenide ones. Reactivities of the elemental chalcogens towards mixed-metal dichalcogenides giving the corresponding trichalcogenide compounds are of the following order: S > Se > Te.

While S can only be found in a triply bridging site in the mixed-chalcogenide, mixed-metal clusters of the type  $\text{Cp}_2\text{Mo}_2\text{Fe}_2(\text{CO})_6\text{E}_2\text{E}'$ , Se and Te can both adopt either the  $\mu_4$ - or the  $\mu_3$ -bonding modes, as seen in the formation of two isomers each of **2** and **3**. Possible interconversion between the two isomeric forms of **3** were investigated. On thermolysis of pure **3a** or **3b** for 2 h, at  $110^\circ\text{C}$ , substantial decomposition occurred, but conversion of one isomer to the other was not observed; pure **3a** and **3b** were recovered from the solutions.

#### Acknowledgements

We are grateful to the Department of Atomic Energy, Government of India, for providing financial support in the form of a research grant to one of us (P.M.).

#### References

- [1] (a) A. Muller, *Polyhedron* 5 (1986) 323. (b) P. Mathur, I.J. Mavunkal, B.H.S. Thimmappa, V.D. Reddy, B.B.S. Shastri, *Proc. Indian Acad. Sci.* 102 (1990) 395. (c) L.C. Roof, J.W. Kolis, *Chem. Rev.* 93 (1993) 1037. (d) J. Wachter, *Angew. Chem. Int. Ed. Engl.* 28 (1989) 1613. (e) K. Tatsumi, H. Kawaguchi, K. Tani, *Angew. Chem. Int. Ed. Engl.* 32 (1993) 591. (f) L. Linford, H.G. Raubenheimer, *Adv. Organomet. Chem.* 32 (1991) 1.
- [2] (a) P. Mathur, I.J. Mavunkal, A.L. Rheingold, *J. Chem. Soc. Chem. Commun.* (1989) 382. (b) W.A. Herrmann, *Angew. Chem. Int. Ed. Engl.* 25 (1986) 56. (c) L.E. Bogan, G.R. Clark, T.B. Rauchfuss, *Inorg. Chem.* 25 (1986) 4050. (d) L.E. Bogan, D.A. Lesch, T.B. Rauchfuss, *J. Organomet. Chem.* 250 (1983) 429. (e) P. Mathur, I.J. Mavunkal, V. Rugmini, M.F. Mahon, *Inorg. Chem.* 29 (1990) 4838. (f) P. Mathur, D. Chakrabarty, M.M. Hossain, V. Rugmini, R.S. Rashid, A.L. Rheingold, *Inorg. Chem.* 31 (1992) 1106. (g) R.D. Adams, *Polyhedron* 4 (1985) 2003.
- [3] (a) K.H. Whitmire, *J. Coord. Chem.* 17 (1988) 95. (b) N.A. Compton, R.J. Errington, N.C. Norman, *Adv. Organomet. Chem.* 31 (1990) 91. (c) P. Mathur, M.M. Hossain, R.S. Rashid, *J. Organomet. Chem.* 460 (1993) 83.
- [4] (a) P. Mathur, D. Chakrabarty, I.J. Mavunkal, *J. Cluster Sci.* 4 (1993) 351. (b) P. Mathur, D. Chakrabarty, M.M. Hossain, *J. Organomet. Chem.* 401 (1991) 167. (c) P. Mathur, M.M. Hossain, S.B. Umbarkar, C.V.V. Satyanarayana, S.S. Tavale, V.G. Puranik, *Organometallics* 14 (1995) 959.
- [5] D.A. Lesch, T.B. Rauchfuss, *Organometallics* 1 (1982) 499.
- [6] (a) P. Braunstein, J.-M. Jud, M. Tiripicchio-Camellini, E. Sappa, *Angew. Chem. Int. Ed. Engl.* 21 (1982) 307. (b) P.D. Williams, M.D. Curtis, D.N. Duffy, W.D. Butler, *Organometallics* 2 (1983) 165.
- [7] P. Mathur, M.M. Hossain, A.L. Rheingold, *Organometallics* 13 (1994) 3909.
- [8] (a) P. Mathur, M.M. Hossain, A.L. Rheingold, *Organometallics* 12 (1993) 5029. (b) P. Mathur, M.M. Hossain, S.B. Umbarkar, C.V.V. Satyanarayana, A.L. Rheingold, L.M. Liable-Sands, G.P.A. Yap, *Organometallics* 15 (1996) 1898.
- [9] D.S. Ginley, C.R. Boch, M.S. Wrighton, *Inorg. Chim. Acta* 23 (1977) 85.
- [10] D. Chakrabarty, M.M. Hossain, R.K. Kumar, P. Mathur, *J. Organomet. Chem.* 410 (1991) 143.
- [11] D.A. Lesch, T.B. Rauchfuss, *Inorg. Chem.* 20 (1981) 3583.
- [12] P. Mathur, D. Chakrabarty, M.M. Hossain, *J. Organomet. Chem.* 420 (1991) 79.
- [13] N. Walker, D. Stewart, *Acta Crystallogr. Sect. A*: 39 (1983) 158.
- [14] G.M. Sheldrick, *Acta Crystallogr. Sect. A*: 46 (1990) 467.
- [15] G.M. Sheldrick, *SHELXL*, A computer program for crystal structure refinement, University of Gottingen, 1993.
- [16] P. McArdle, *J Appl. Crystallogr.* 27 (1994) 438.
- [17] L.E. Bogan, T.B. Rauchfuss, A.L. Rheingold, *J. Am. Chem. Soc.* 107 (1985) 3843.